NACA

RESEARCH MEMORANDUM

DAMPING IN ROLL OF MODELS WITH 45°, 60°, AND 70° DELTA WINGS DETERMINED AT HIGH SUBSONIC, TRANSONIC, AND SUPERSONIC SPEEDS WITH ROCKET-POWERED MODELS

By E. Claude Sanders, Jr.

Langley Aeronautical Laboratory
Langley Field, Va.

NATIONAL ADVISORY COMMITTEE
FOR AERONAUTICS

WASHINGTON
June 25, 1952

NATIONAL ADVISORY COMMITTEE FOR AERONAUTICS

RESEARCH MEMORANDUM

DAMPING IN ROLL OF MODELS WITH 45°, 60°, AND 70° DELTA WINGS DETERMINED AT HIGH SUBSONIC, TRANSONIC, AND SUPERSONIC SPEEDS WITH ROCKET-POWERED MODELS

By E. Claude Sanders, Jr.

SUMMARY

Rocket-powered models with three- and four-wing arrangements have been flown to determine the damping in roll at zero lift of some delta wings which were swept 45°, 60°, and 70° at the leading edge and had NACA 65A006 and hexagonal airfoil sections. The Mach number range of these tests was from 0.7 to 1.5. Damping in roll decreased with an increase in leading-edge sweep angle and also decreased with an increase in the number of wings at leading-edge sweep angles of 60° or larger. Theoretical data were consistently higher than experimental data. The total drag coefficient was obtained at zero lift for all the models tested.

INTRODUCTION

The National Advisory Committee for Aeronautics has devised a simplified rocket-model technique (ref. 1) utilizing canted nozzles to produce a torque, which allows a determination of damping in roll at high subsonic, transonic, and supersonic speeds at high Reynolds numbers. This technique has been utilized in an investigation to determine the damping-in-roll characteristics of configurations with three- and four-wing arrangements. The wings, of triangular plan form and swept 45°, 60°, and 70° at the leading edge, had NACA 65A006 and constant-thickness hexagonal airfoil sections parallel to the model center line. The wings were mounted on bodies similar to those described in reference 1.

The damping-in-roll and total drag coefficients were obtained for each configuration at zero lift through a Mach number range of approximately 0.7 to 1.5 corresponding to Reynolds numbers from approximately 4×10^6 to 17×10^6 with the exception of the configuration which had

the 70° swept wing and hexagonal airfoil section. This configuration was flown to a Mach number of approximately 2.1 corresponding to a Reynolds number of approximately 28×10^6. The models were tested in flight at the Langley Pilotless Aircraft Research Station at Wallops Island, Va.

SYMBOLS

C_l rolling-moment coefficient, $\frac{L}{qS_n b}$

C_{l_p} damping-in-roll derivative, $\frac{\Delta C_l}{\frac{pb}{\Delta 2V}}$

$\beta = \sqrt{M^2 - 1}$

C_D total-drag coefficient, $\frac{D}{qS_{e_n}}$

D total drag, lb

L rolling moment, ft-lb

L_o out-of-trim rolling moment, ft-lb

T torque, lb-ft

p rolling angular velocity, radians/sec

$\dot{p}$ rolling angular acceleration, radians/sec^2

V forward velocity, ft/sec

q dynamic pressure, lb/sq ft

M Mach number

A aspect ratio, $\frac{b^2}{S_n}$ $(n = 2)$

R Reynolds number, based on the mean aerodynamic chord of wing (wing assumed to extend to model center line)

Λ angle of sweep of wing leading edge, deg

b	wing span (diameter of circle generated by wing tips), ft
d	maximum diameter of body, ft
S_n	n times the area of semispan wing (wing assumed to extend to model center line), sq ft
S_{e_n}	n times the exposed area semispan wing (wing assumed to extend to wing-body juncture), sq ft
I_X	moment of inertia about longitudinal axis, slug-ft^2
m	ratio of the tangent of the semi-vertex angle of the delta plan form to the tangent of the Mach angle, $\frac{\tan \epsilon}{\tan \mu}$

Subscripts:

1	sustainer-on flight
2	coasting flight
n	number of wings

MODELS

The models used in this investigation were similar to those used in reference 1, except for wing design. The body consisted of a cylindrical wooden fuselage with a spinsonde nose section (ref. 2) and incorporated a sustaining rocket motor with canted nozzles. The test wings, made of laminated spruce, had an alluminum-alloy center line stiffener and a skin stiffener made of steel shim stock and were attached near the rear of the basic fuselage in three- or four-wing arrangements. The wing arrangement and the distance of the trailing edge of the wing from the rear of the model for the various configurations are shown in figure 1. Also shown in figure 1 is a sketch of a typical model and a table of pertinent wing geometry. Six of the configurations flown in this investigation had wings with NACA 65A006 airfoil sections parallel to the model center line. There were three configurations with leading-edge sweep angles of 45°, 60°, and 70°, respectively, for each of the two wing arrangements. Two other delta-wing plan forms tested and included in this paper had hexagonal airfoils of constant thickness. One of these plan forms had a three-wing arrangement with a leading-edge sweep of 60° and a thickness ratio of 3 percent at the wing-body juncture which increases to 9 percent at the tip end of the flat-sided part.

The other plan form had a four-wing arrangement with a leading-edge sweep of 70° and a thickness ratio of approximately 1.8 percent at the wing-body juncture increasing to 5.4 percent at the tip end of the flat-sided part. This latter configuration had a modified delta-wing plan form. A sketch of the wings tested is shown in figure 2 and photographs of two of the test configurations are presented as figure 3. Two models of each configuration were flown to insure that complete data were obtained.

TEST PROCEDURE AND APPARATUS

Each model was launched from a rail-type launcher at an elevation angle of approximately 70° to the horizontal and was accelerated to a Mach number of approximately 0.7 by means of a booster rocket motor which separated from the model when its fuel was exhausted. The model was then accelerated by an internal rocket motor with canted nozzles to a Mach number of approximately 1.5. Thus, a Mach number range of about 0.7 to 1.5 was covered corresponding to a Reynolds number range of approximately 4×10^6 to 17×10^6 based on the mean aerodynamic chord of the wing. In order to extend the Mach number range through which data were desired for the wing of a specific missile configuration (70° modified delta), the second model of that configuration was equipped with a more powerful booster rocket motor to attain a Mach number of approximately 2.1 corresponding to a Reynolds number of approximately 28×10^6 based on the mean aerodynamic chord of the wing. The rate of roll and rolling acceleration were obtained by means of a spinsonde (ref. 2) contained in the nose of the model. The flight path velocity and longitudinal acceleration were obtained with a C. W. Doppler radar set. Atmospheric measurements covering the altitude range of flight tests were obtained with radiosondes.

REDUCTION OF DATA

The damping-in-roll derivative was calculated by balancing the moments acting on the model. The torque nozzle and wing misalinement produced rolling moments which were balanced by the inertia moment and the damping moment produced by the wing and body. Moment equilibrium for one degree of freedom may be written:

$$I_X \dot{p} - \frac{\partial L}{\partial p} p = T + L_0 \qquad (1)$$

Resolving equation (1) into coefficient form at the same Mach number for the accelerated and the decelerated parts of flight and solving them simultaneously for the damping-in-roll derivative yields:

$$-C_{l_p} = \frac{\frac{T}{q_1} - \left(\frac{I_{X_1}\dot{p}_1}{q_1} - \frac{I_{X_2}\dot{p}_2}{q_2}\right)}{\frac{S_n b^2}{2}\left(\frac{p_1}{V_1} - \frac{p_2}{V_2}\right)} \tag{2}$$

The complete analysis of this method for determining the damping-in-roll derivative may be found in reference 1.

The accuracy of C_{l_p}, $C_{\dot{p}}$, and their component errors for these tests are estimated to be within the following limits:

Torque, T, lb-ft	±2.50
Rolling angular velocity, radians/sec	±1.00
Damping-in-roll derivative	±0.03
Total-drag coefficient, C_D	±0.002
Mach number, M	±0.010

The preceding estimations are based on individual model calculations. The agreement between results obtained for individual models in reference 1 was better than the estimated accuracy indicated for individual models in the high subsonic and supersonic speed ranges. However, the relative magnitudes of the lateral-trim changes between duplicate models may affect the repeatability of p and, consequently, C_{l_p} throughout the Mach numbers at which this trim change is effective. In the present investigation only configuration 7 had an indication of a trim change in the basic-roll data. A more complete analysis of factors producing the error in C_{l_p} is reported in reference 1.

RESULTS AND DISCUSSION

Damping in Roll

The variation with Mach number of damping in roll of missile configurations with delta-wing plan forms is presented in figure 4. Shown in figure 4(a) are the data from configurations with the three-wing arrangement. Damping in roll decreased with an increase in the leading-edge sweep angle as was previously shown in references 3 and 4. The

configuration with the 45° delta wing had a 28-percent reduction in C_{l_p} from Mach number 1.0 to Mach number 1.5, whereas C_{l_p} for the other two configurations decreased less in this range.

In figure 4(b) is presented the damping-in-roll data for the configurations with the four-wing arrangement. The damping in roll for these configurations shows about the same general trend as that for configurations with wings of corresponding sweep angles in the three-wing arrangement (fig. 4(a)). The damping in roll was lower for the configurations with the four-wing arrangement than for the configurations with the three-wing arrangement in the case of the 60° and 70° wings but was about the same for configurations with either wing arrangement in the case of the 45° wing. None of the data in figures 4(a) and 4(b), which are for models with NACA 65A006 airfoil sections, exhibited any wing dropping tendencies (ref. 5).

The damping-in-roll data for the models with 60° and 70° delta wings with the hexagonal airfoil sections are presented in figure 4(c). In the lower plot the Mach number range is extended to include the higher Mach number data for configurations 7 and 8. Configuration 7 (60° delta wing) has a three-wing arrangement and a thickness ratio of 3 percent at the wing-body juncture which increases to 9 percent at the tip end of the flat-sided part. The damping in roll in the supersonic range for this configuration was slightly higher than that for configuration 2 which was identical except for airfoil section and thickness ratio. There was an indication of wing dropping (ref. 5) around Mach number 0.9 in the basic roll data of configuration 7, and it is reflected in the C_{l_p} data. Also shown for comparison in figure 4(c) is the damping in roll for a cruciform missile configuration (ref. 6) with 60° delta wings which were similar to those of configuration 7. The C_{l_p} from reference 6 (four-wing arrangement) is slightly lower in the supersonic range than the C_{l_p} for configuration 7 (three-wing arrangement). This relation was also shown for configurations 2 and 5 which differed from each other only in the number of wings.

Configuration 8 (70° modified wing) had a four-wing arrangement and a thickness ratio of 1.8 percent at the wing-body juncture which increases to 5.4 percent at the tip end of the flat-sided part. The damping in roll for configuration 8 is lower than that from reference 6. This condition is due partly to the increase in leading-edge sweep angle and to the modified plan form. The smaller thickness ratio of configuration 8 would tend to increase its damping in roll over that of reference 6, but apparently was not effective enough to overcome the effect of the sweep and the modified plan form.

At subsonic speeds, the experimental damping in roll was less than the theoretical value of $\frac{\pi A}{32}$. A comparison of the experimental and theoretical damping in roll at supersonic speeds for all of the wings tested is shown in figure 5. The theoretical curve for the four-wing arrangement was reported in reference 7. The theoretical curve for the three-wing arrangement is a mean line between the theoretical curves for the two-wing and the four-wing arrangement as is indicated in reference 7.

In figure 5 the theoretical values of C_{l_p} are higher than experimental values. This difference, which has been noticed in previous investigations of damping-in-roll characteristics of other wing plan forms (ref. 1), is believed to be due to the combined effects of body influence, section thickness, and wing twisting which were not taken into consideration in the theory for isolated wings (ref. 7). The body influence is very small in the range of body diameter to wing span ratios in which these wings were tested as shown in references 8 and 9. Thickness reduces the C_{l_p} (ref. 10) as compared to theory which is based on an infinitely thin wing. There has been no correction applied to the present experimental data for wing twisting; however, these wings are believed to be near the rigid case with a maximum loss of C_{l_p} due to twisting of the order of 10 percent. The reduction in experimental damping in roll with an increase in the number of wings in the case of the configurations with 60° and 70° delta wings (figs. 4(a) and 4(b)) is believed to be due to the effects of mutual interference between wings (ref. 9) and is of the same magnitude as predicted by theory (ref. 7) which includes interference effects. Unlike the 60° and 70° delta-wing configurations, the 45° delta-wing configuration had approximately the same damping in roll at supersonic speeds for both wing arrangements (figs. 4(a) and 4(b)), an indication of a negligible effect of mutual interference. It can be seen in figure 5 that the experimental results show better agreement with theoretical values as the leading-edge sweep angle increases or as the Mach number decreases ($m \rightarrow 0$).

Drag

The variation of total drag coefficient at zero lift with Mach number is presented in figure 6. A drag rise begins between Mach number of 0.9 and 0.95 for all the configurations with NACA 65A006 airfoil sections and at a lower Mach number for configurations with the hexagonal airfoil sections. The body drag is not known; therefore, the total drag coefficient, which is based on exposed area, can be compared only for the configurations in figure 6(a) and the configurations in figure 6(b) since the exposed area was held constant for each of these

sets of configurations. Comparisons of C_D for these configurations show a decrease in drag with an increase in the leading-edge sweep angle at supersonic speeds for both the three- and four-wing arrangements.

CONCLUSIONS

Damping-in-roll tests have been made of configurations with 45°, 60°, and 70° delta wings in three- and four-wing arrangements with NACA 65A006 and hexagonal airfoil sections and the results have been compared. The following conclusions were drawn from these comparisons:

1. Damping in roll decreased with an increase in leading-edge sweep angle.

2. Damping in roll decreased with an increase in the number of wings for wings with leading-edge sweep angles of 60° or larger. Increasing the number of wings had no apparent effect on the damping in roll of the configurations with wings swept 45° at the leading edge.

3. Theoretical values of damping in roll were higher than experimental values of damping in roll but agreement improved with an increase in leading-edge sweep angle.

Langley Aeronautical Laboratory
National Advisory Committee for Aeronautics
Langley Field, Va.

REFERENCES

1. Edmondson, James L., and Sanders, E. Claude, Jr.: A Free-Flight Technique for Measuring Damping in Roll by Use of Rocket-Powered Models and Some Initial Results for Rectangular Wings. NACA RM L9I01, 1949.

2. Harris, Orville R.: Determination of the Rate of Roll of Pilotless Aircraft Research Models by Means of Polarized Radio Waves. NACA TN 2023, 1950.

3. Sanders, E. Claude, Jr.: Damping in Roll of Straight and 45° Swept Wings of Various Taper Ratios Determined at High Subsonic, Transonic, and Supersonic Speeds With Rocket-Powered Models. NACA RM L51H14, 1951.

4. Sanders, E. Claude, Jr., and Edmondson, James L.: Damping in Roll of Rocket-Powered Test Vehicles Having Swept, Tapered Wings of Low Aspect Ratio. NACA RM L51G06, 1951.

5. Stone, David G.: Wing-Dropping Characteristics of Some Straight and Swept Wings at Transonic Speeds as Determined With Rocket-Powered Models. NACA RM L50C01, 1950.

6. Martz, C. William, and Church, James D.: Flight Investigation at Subsonic, Transonic, and Supersonic Velocities of the Hinge-Moment Characteristics, Lateral-Control Effectiveness, and Wing Damping in Roll of a 60° Sweptback Delta Wing With Half-Delta Tip Ailerons. NACA RM L51G18, 1951.

7. Ribner, Herbert S.: Damping in Roll of Cruciform and Some Related Delta Wings at Supersonic Speeds. NACA TN 2285, 1951.

8. Tucker, Warren A., and Piland, Robert O.: Estimation of the Damping in Roll of Supersonic-Leading-Edge Wing-Body Combinations. NACA TN 2151, 1950.

9. Bland, William M., Jr., and Dietz, Albert E.: Some Effects of Fuselage Interference, Wing Interference, and Sweepback on the Damping in Roll of Untapered Wings as Determined by Techniques Employing Rocket-Propelled Vehicles. NACA RM L51D25, 1951.

10. Edmondson, James L.: Damping in Roll of Rectangular Wings of Several Aspect Ratios and NACA 65A-Series Airfoil Sections of Several Thickness Ratios at Transonic and Supersonic Speeds as Determined With Rocket-Powered Models. NACA RM L50E26, 1950.

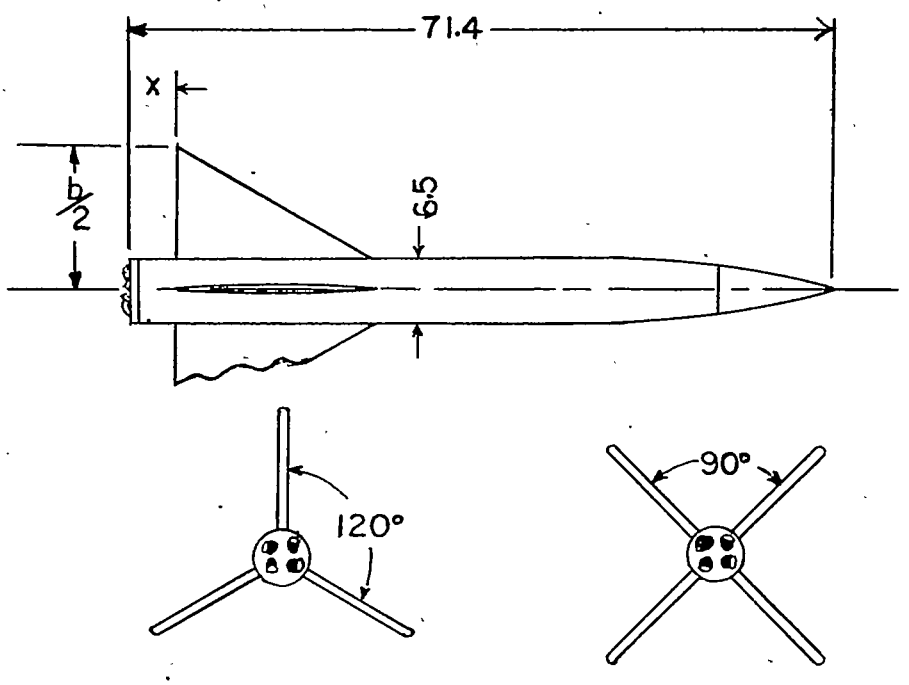

Configurations 1,2,3,7 Configurations 4,5,6,8

NACA

Wing arrangement

Configuration	Number of wings	Wing area, S_n	Sweep of L.E.	A	Airfoil section	Reynolds number (10^{-6})	x
1	3	3.83	45°	4.00	NACA 65A006	5.2 to 10.0	4.73
2	3	4.25	60°	2.31		5.2 to 13.3	4.73
3	3	4.73	70°	1.45		6.2 to 16.9	3.02
4	4	5.11	45°	4.00		3.8 to 9.3	4.73
5	4	5.67	60°	2.31		5.9 to 13.3	4.73
6	4	6.31	70°	1.45		4.1 to 9.2	3.02
7	3	3.74	60°	2.31	Hexagonal 0.03 to 0.09	4.5 to 13.6	4.73
8	4	8.63	70°	1.45	Hexagonal 0.018 to 0.054	8.8 to 27.5	3.02

Figure 1.- General arrangement of models and a table of pertinent wing geometry. All dimensions are in inches.

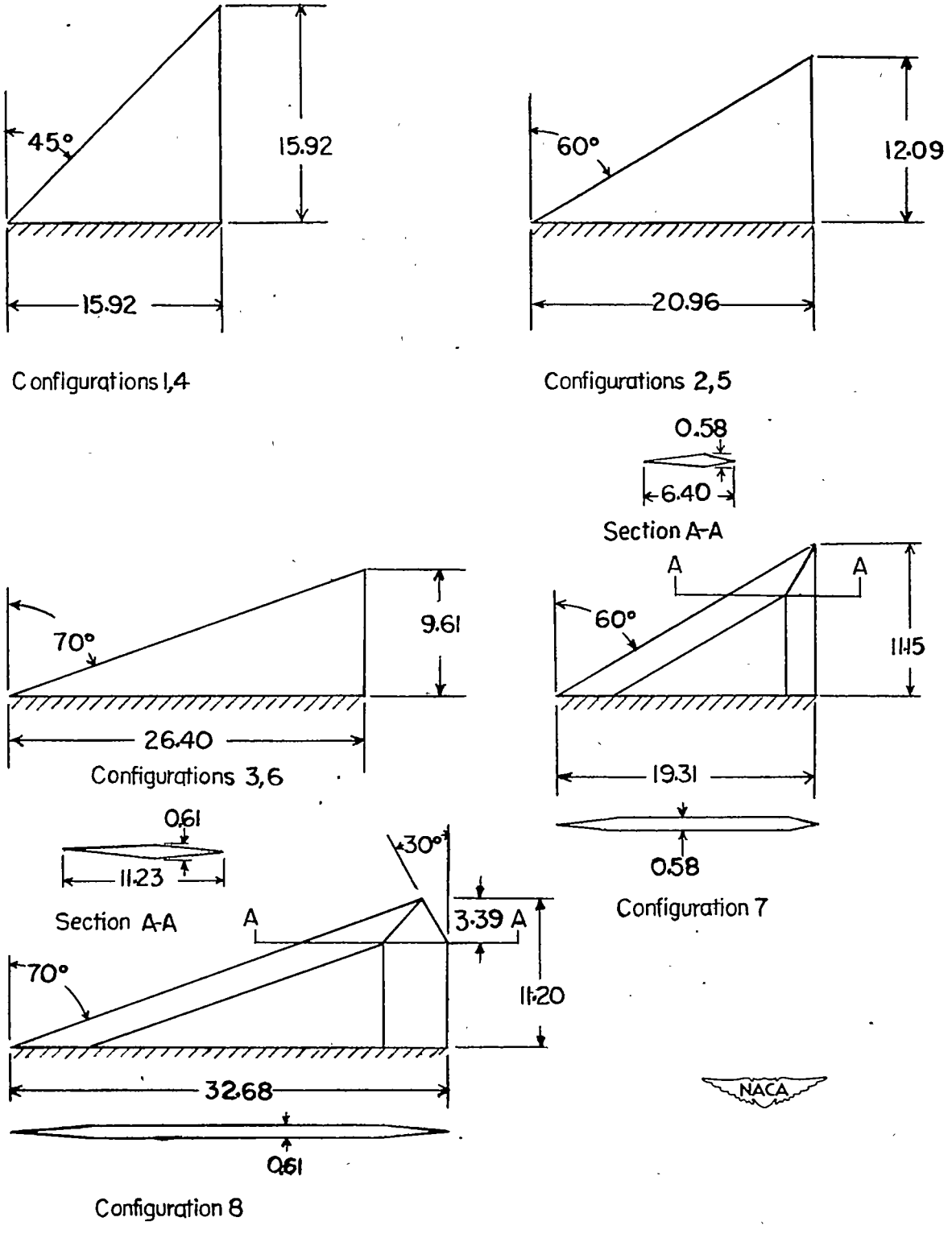

Figure 2.- Physical properties of test wings. All dimensions are in inches.

(a) Configuration 5.

Figure 3.- Typical models with four-wing arrangement.

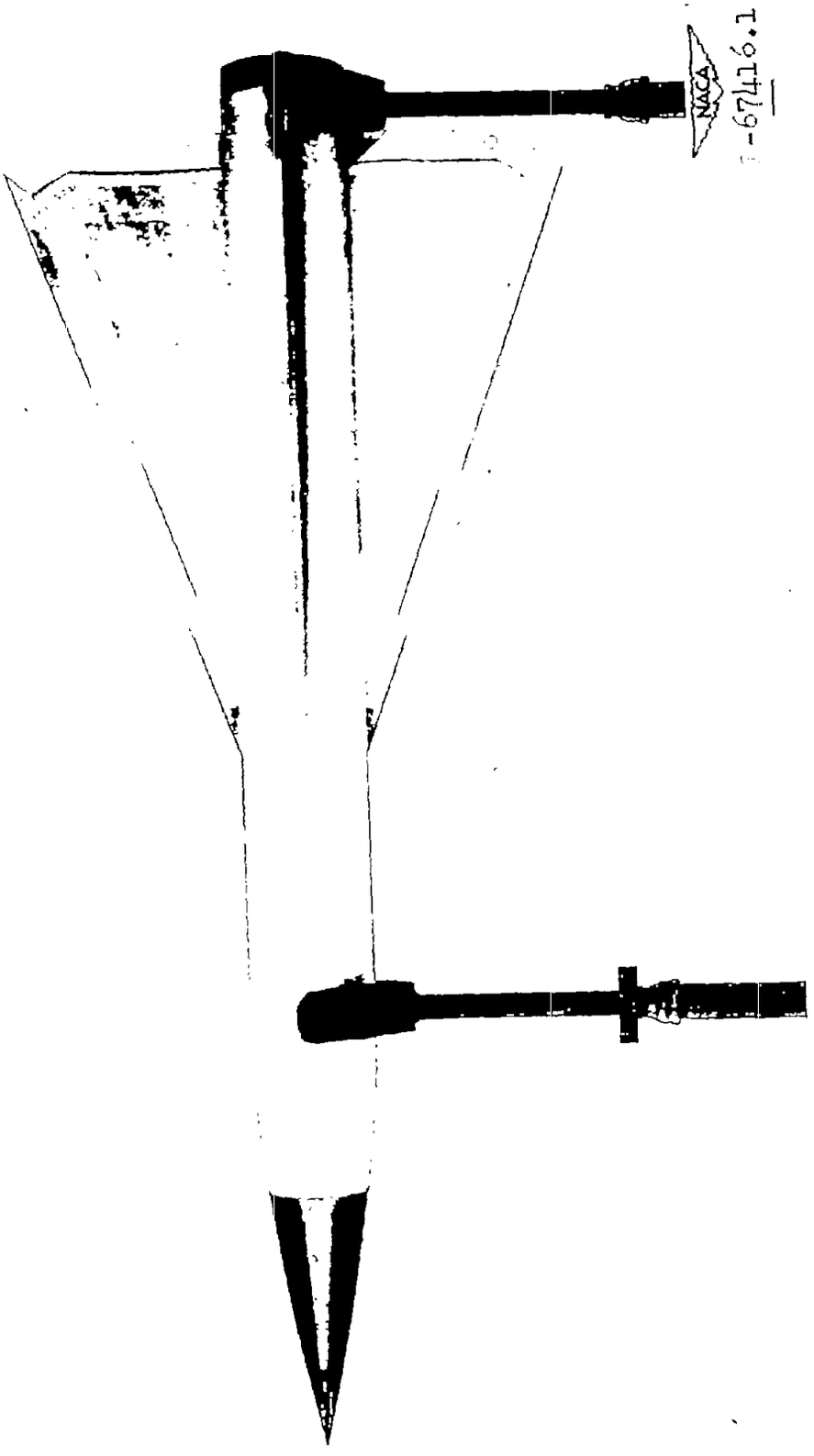

(b) Configuration 8.

Figure 3.- Concluded.

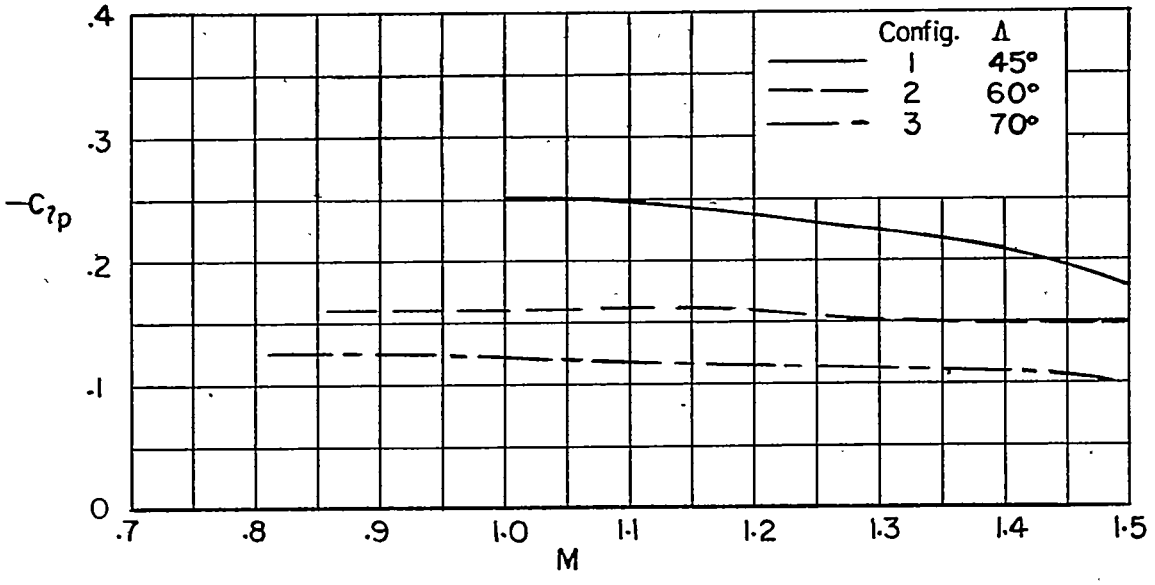

(a) Three-wing arrangement. NACA 65A006 airfoil section.

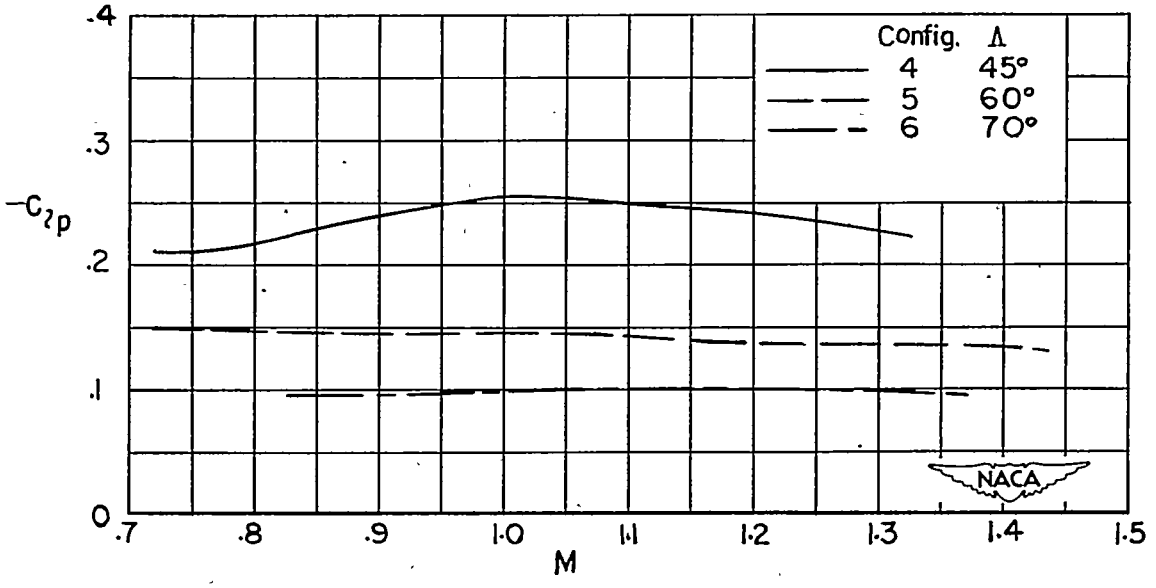

(b) Four-wing arrangement. NACA 65A006 airfoil section.

Figure 4.- Variation with Mach number of damping in roll of missile configurations with delta-wing plan forms.

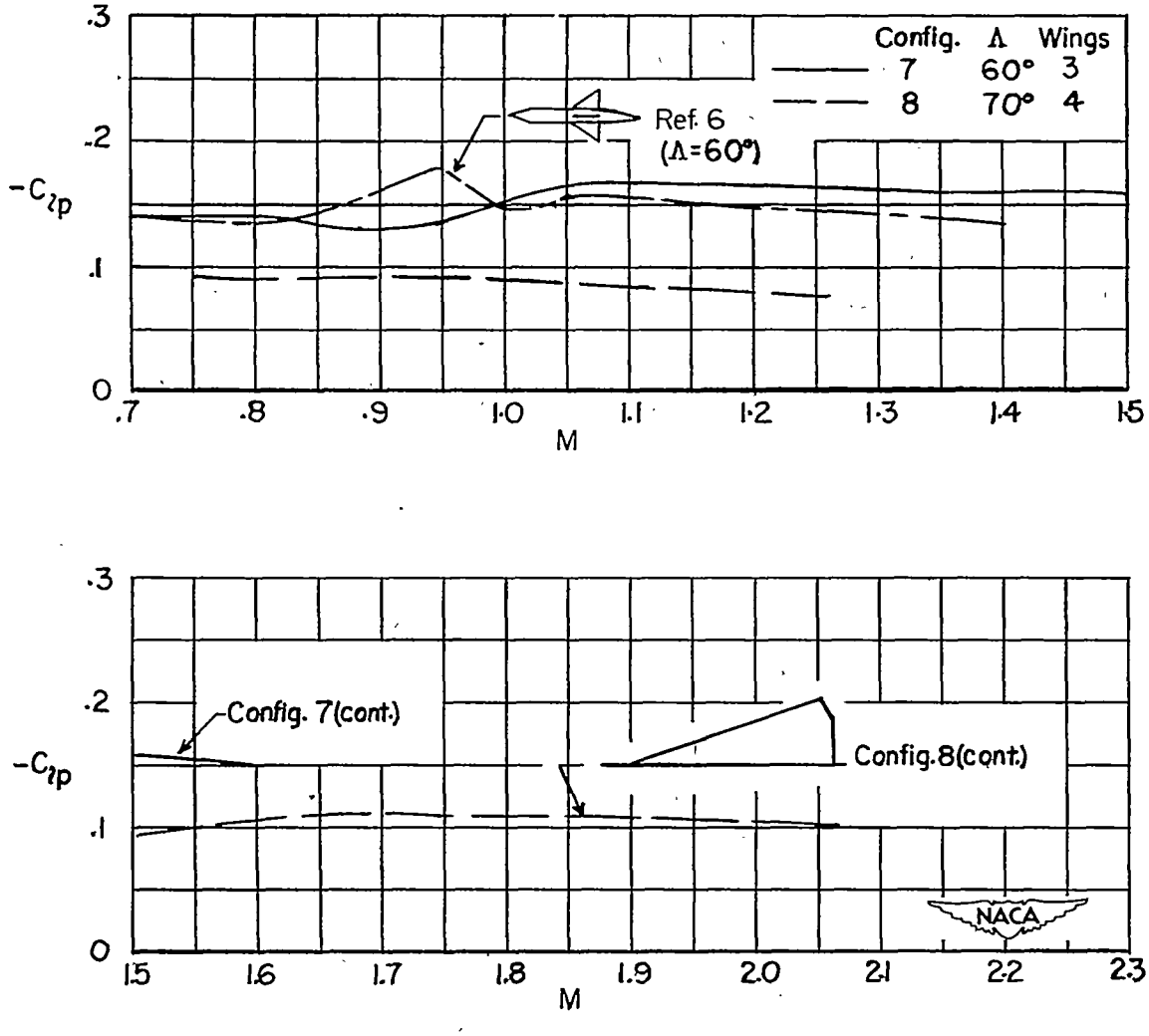

(c) Three- and four-wing arrangements. Hexagonal airfoil sections.

Figure 4.- Concluded.

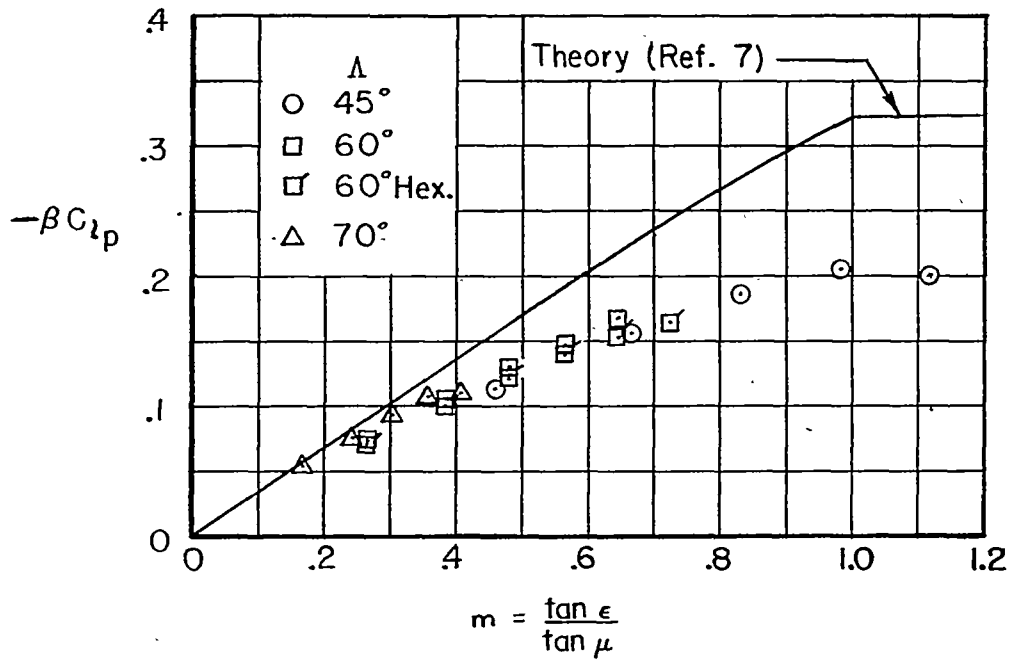

(a) Three-wing arrangement.

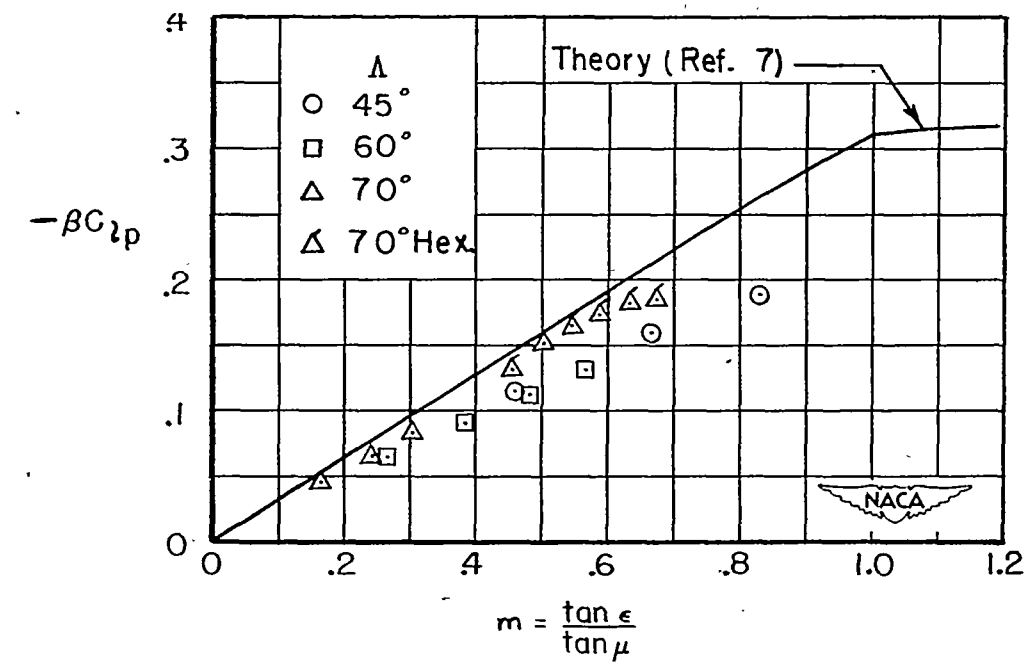

(b) Four-wing arrangement.

Figure 5.- Comparison of experimental C_{l_p} with theory for delta wings.

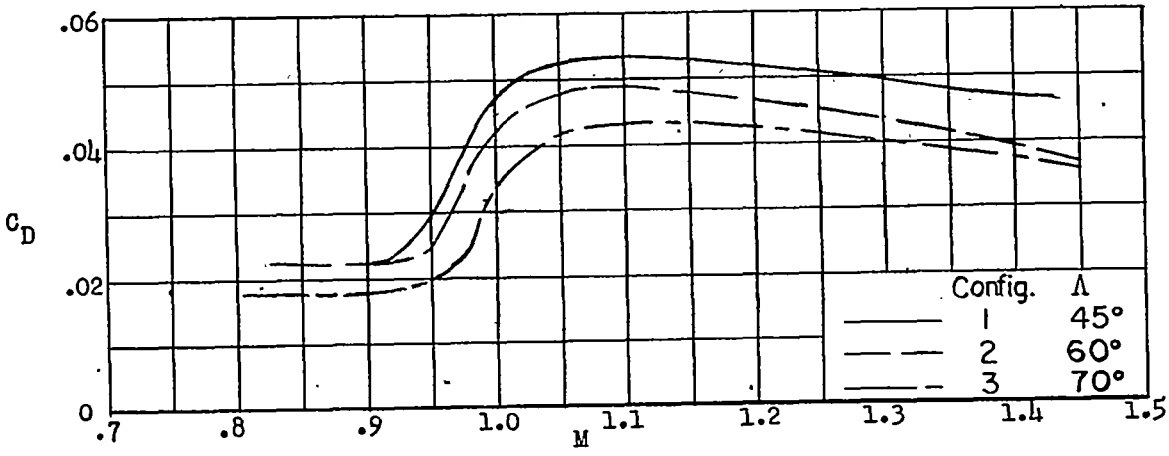

(a) Three-wing arrangement. NACA 65A006 airfoil section.

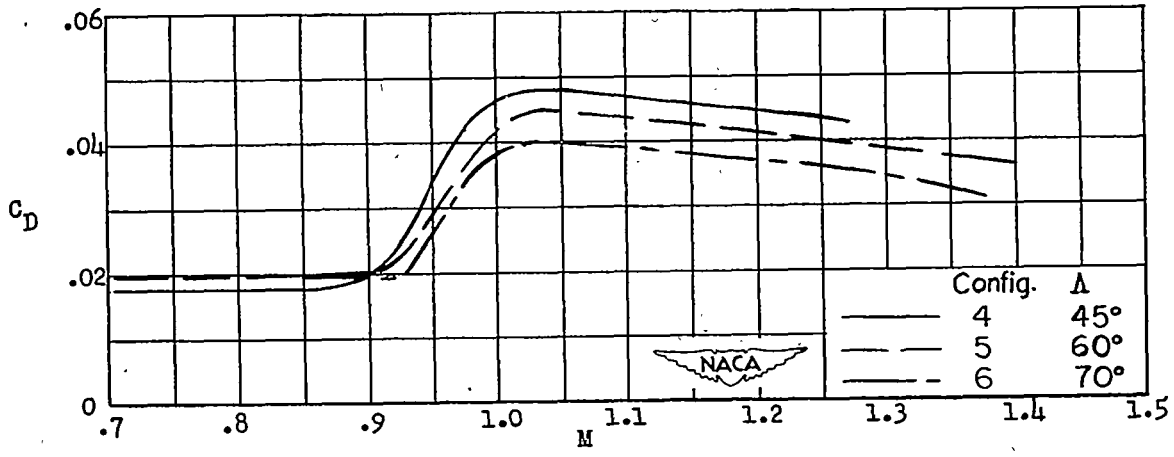

(b) Four-wing arrangement. NACA 65A006 airfoil section.

Figure 6.- Variation of total drag coefficient at zero lift with Mach number.

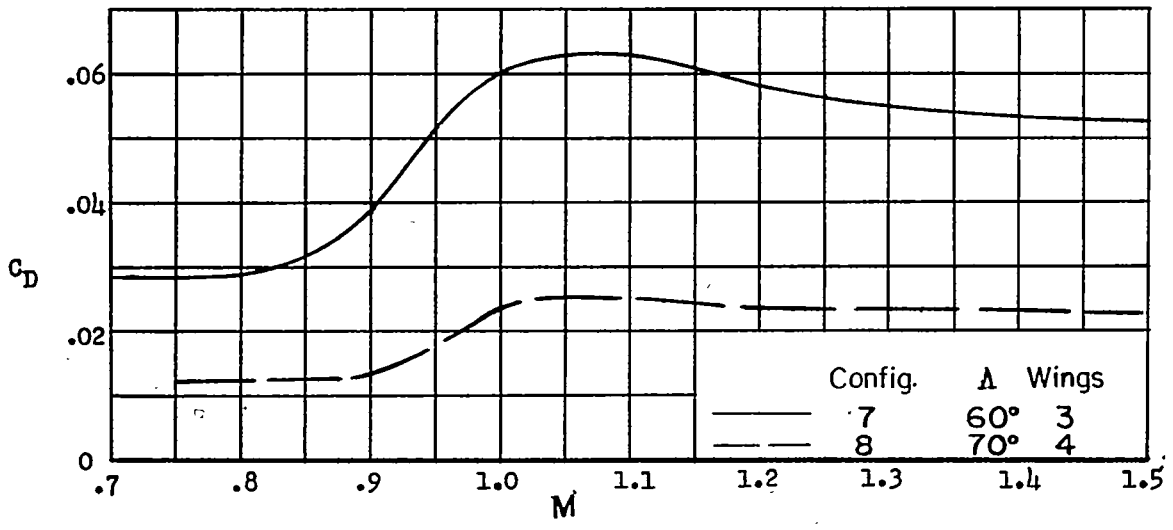

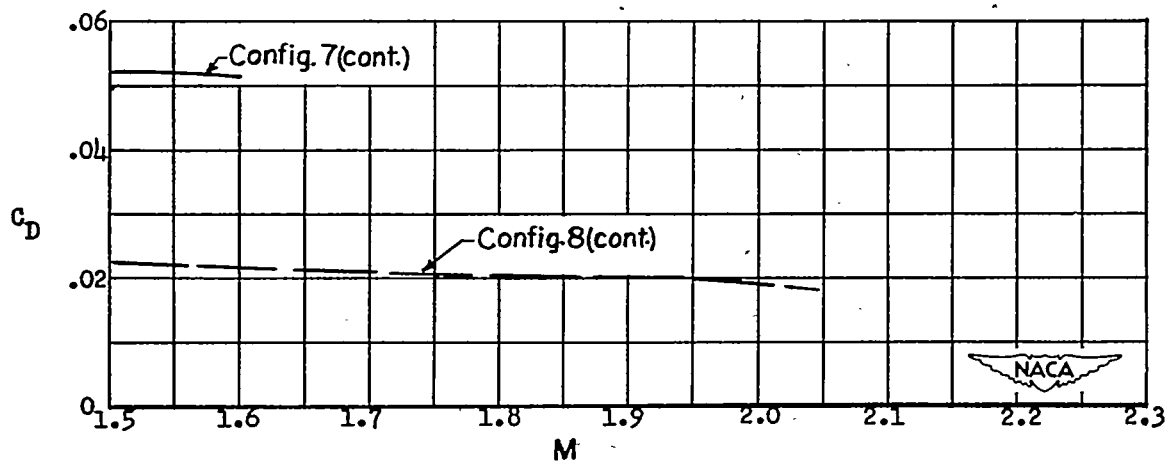

(c) Three- and four-wing arrangement. Hexagonal airfoil section.

Figure 6.- Concluded.

NACA-Langley - 6-20-52 -325